Title

Seismic Response of Rail Embankments

Authors

Yarahuaman, Axel

McCartney, John S

Publication Date

2022-03-17

DOI

10.1061/9780784484067.031

Peer reviewed

Seismic Response of Rail Embankments

Axel Yarahuaman[1], S.M. ASCE; and John S. McCartney[2], Ph.D., P.E., F.ASCE

[1]Graduate Research Assistant, Department of Structural Engineering, University of California, San Diego, La Jolla, CA 92093-0085; Email: ayarahua@ucsd.edu
[2]Professor and Chair, Department of Structural Engineering, University of California, San Diego, La Jolla, CA 92093-0085; Email: mccartney@ucsd.edu

ABSTRACT

This paper presents an evaluation of the seismic response of a full-scale rail embankment tested on the University of California San Diego (UCSD) Powell Laboratory shake table. The goal of performing the experiment was to understand the impacts of earthquake motions on the seismic settlement of the embankment and the associated crosslevel variation of the rails. The tested specimen consisted of a half-section embankment consisting of layers of compacted ballast, subballast, and clay subgrade having a total height of 1.50 m and a length in the direction of shaking of 7.52 m to accommodate typical rail embankment slope angles. The specimen had a width of 3.5 m that permitted 5 ties to be connected to the rails. After characterizing the dynamic deformation response of the container designed, a rail embankment specimen was constructed and tested under an actual earthquake motion. The applied motion induced a maximum horizontal rail acceleration of 1.38 g but only a small residual crosslevel variation of only 0.66 mm was measured.

INTRODUCTION

The San Francisco Bay Area Rapid Transit District (BART) is a heavy-rail public transit system that links the San Francisco Peninsula with Eastern Bay and Southern Bay communities. The BART system includes up to 210 km of track and 50 stations an accommodated an average of 405,000 trips on weekdays before the COVID-19 pandemic (BART 2020). As the San Francisco Bay Area is in a highly seismic region, earthquakes pose an important hazard to BART's rail infrastructure, which relies mostly on ballasted tracks. Several reported observations from past earthquakes indicate the disruption of track operation due to the distortion of track geometrical parameters (Housner and Lili 2014), emphasizing the need to predict the possible effects of earthquake-induced deformations on the track uniformity. BART categorizes rail tracks in five classes based on uniformity, with the main criteria for uniformity being the "crosslevel variation" (CLV). The CLV is defined as the differential elevation between rails, and an implication of greater CLV values is that trains should operate at slower speeds. The optimal performance of the rail system is Class 5, which allows speeds of up to 129 km/h but requires a CLV less than 19.05 mm. During earthquakes, it is possible that the two rails in a track may settle differentially due to the presence of the free face of the rail embankment slope, leading to an increase in CLV and a change in track class. Although some studies have focused on the lateral deformation of single-direction ballasted rail embankments and the impacts on rail buckling (e.g., Nakamura et al. 2011; Sogabe et al. 2013), there is not a significant experimental database available in the literature focused on the dynamic settlement response of 2-direction ballasted rail embankments during earthquakes.

Accordingly, a research project at UCSD is underway to characterize the relationship between the CLV of ballasted rail tracks and different characteristics of earthquake motions, including the peak ground acceleration (PGA) and the predominant frequency of the earthquake motion with respect to the resonant frequency of the rail embankment. This paper presents the details of a plane-strain shake table experiment on a full-scale rail embankment section performed as part of this broader research project, along with key measurements from a typical earthquake motion.

CONCEPTUAL EXPERIMENTAL DESIGN

To identify a representative cross-section of a ballasted rail embankment for testing on the UCSD Powell Laboratory shake table, as-built plans from several BART rail lines were evaluated, including the Southern Alameda County Line, the Berkeley-Richmond Line, and the Central Costa Line. An example of a typical rail embankment section along the Southern Alameda County Line is shown in Figure 1. The rail embankment section includes two directions of rail overlying a layer of ballast, which is overlying a layer of subballast and a layer of subgrade soil (labeled as the "embankment" layer in Figure 1). The geometries of the ballast and subballast layers are constant along the length of the rail line while the subgrade layer thickness varies along the length of the rail line. The interface between the subballast and subgrade has a 24:1 slope, while the unconstrained slope boundaries of the ballast and subgrade layers follow 2:1 slope.

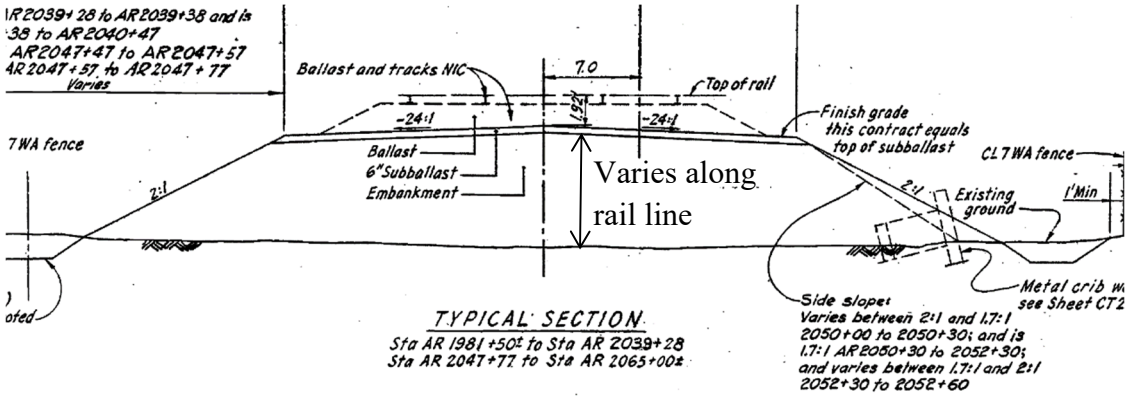

Figure 1. 2-direction rail embankment section from the Southern Alameda County Line.

Although earthquakes may occur in any direction, this study focuses on horizontal shaking perpendicular to the direction of the train or to the left and right in the rail cross-section to characterize the CLV. Some simplifications to the geometry of the typical rail embankment section were necessary so that a full-scale specimen could be tested within the capabilities of the UCSD Powell Laboratory shake table. The shake table consists of a 16-mm thick steel deck plate with a length of 4.9 m in the direction of shaking and a width of 3.1 m in the direction perpendicular to shaking. The table moves over two stationary shafts driven by a single fatigue-rated double-acting hydraulic actuator with a dynamic capacity of 405 kN and a total dynamic stroke of 305 mm (Trautner et al. 2017). The shake table was designed for a maximum vertical payload of 350 kN and a moment capacity of 420 kN-m. The example rail embankment section in Figure 1 has a maximum height of 3.4 m and a width of 21.8 m at the base of the subgrade layer, which is too heavy and long to accommodate atop the shake table. Accordingly, a rail embankment specimen was defined to have half the width of the typical rail embankment with a subgrade layer thickness that was as thick as possible to maximize possible amplification and minimize any bottom

boundary effects, but thin enough that the total weight would be close to the maximum payload of the shake table and that the length of the specimen would have a length that could fit on a table extension. The length of the specimen is linked to the height through the required slopes of the ballast, subballast and subgrade layers. The geometry of the selected rail embankment specimen shown in Figure 2 has a height of 1.50 m and a length of 7.52 m. Further, a width of 3.5 m was selected which permits five ties to be connected to the rail. The selected rail embankment specimen has a weight of approximately 550 kN (container weight not included). Although the weight surpasses the recommended capacity of the shake table by about 35%, previous tests have also been performed on this range of payloads (e.g., Zheng et al. 2019; Zayed et al. 2020).

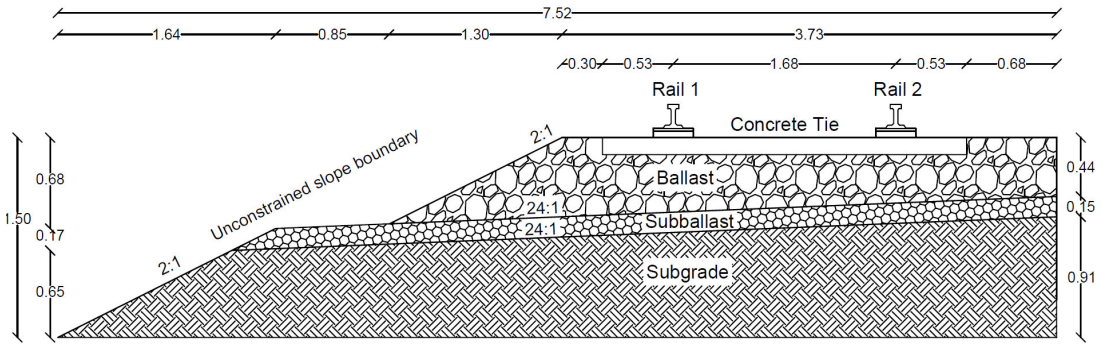

Figure 2. Specimen configuration selected for the full-scale rail embankment tests.

Soil Characterization

In a ballasted rail embankment, the ballast consists of coarse aggregates that is the primary load-bearing platform supporting the track superstructure, the subballast layer acts as a filter and separator between the ballast and subgrade, and the subgrade consists of a compacted soil with sufficient bearing capacity to resist vehicle loading that is used to bring the rail superstructure to the appropriate grade. This section describes the characterization of the three soil layers used to construct the rail embankment specimen. The ballast layer is 4A AREMA stone provided by Vulcan Materials from a quarry located in Chula Vista, CA. The subballast layer is ¾" (19.05 mm) Class 2 base material also provided by Vulcan Materials from a quarry located in Chula Vista, CA. The subgrade layer is SW-SC well-graded sand with clay and gravel, with low plasticity clay as fines, and was provided by Pacific Clay Products from a quarry located near Riverside, CA. The materials used as the ballast and subballast in this study satisfy the gradation curve requirements in the BART specifications (BART 2009) as shown in Figures 3(a) and 3(b). A dry density of 1469 kg/m^3 of the ballast after vibratory compaction was obtained following ASTM C29 (ASTM 2017), which was used as a target in embankment construction. The maximum dry density of the subballast is 2263 kg/m^3 and was obtained following procedure C of ASTM D698 (ASTM 2000). The subgrade material used in this study satisfies the gradation and Atterberg limits required by BART specifications (BART 2009) necessary for use as subgrade common fill and embankment fill, as shown in Figure 4(a). The subgrade soil is composed by 19% gravel, 75% sand, and 5% fines, which have liquid and plastic limits of 36 and 21, respectively. A maximum dry density of 1775 kg/m^3 and optimum gravimetric water content of 16% were obtained from the compaction curve corresponding to the standard Proctor compaction effort for the subgrade soil and are shown in Figure 4(b).

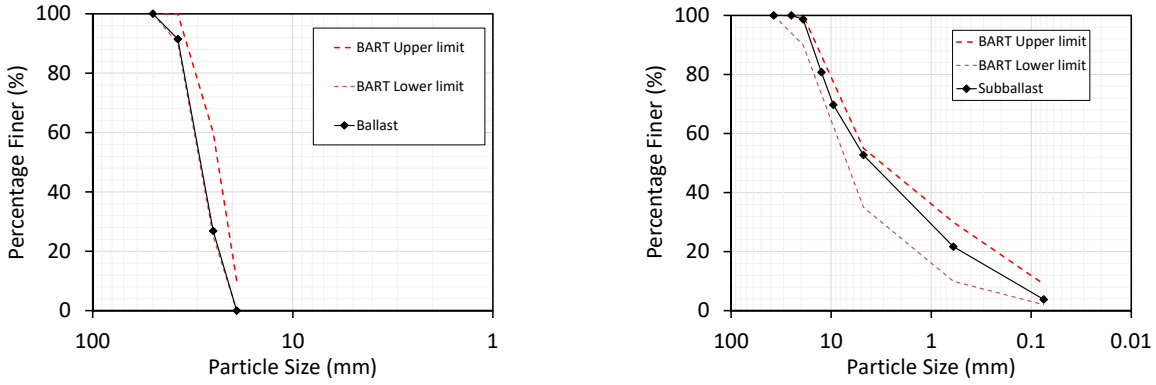

Figure 3. Gradation curves: (a) Ballast; (b) Subballast.

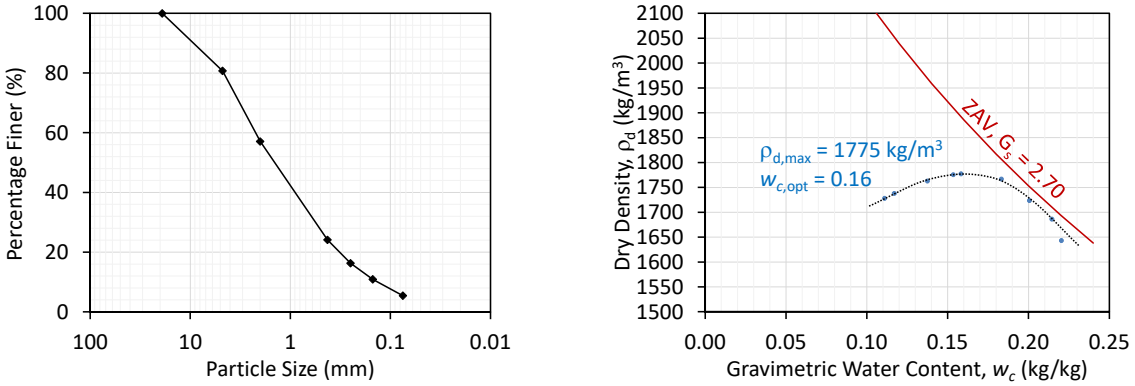

Figure 4. Subgrade material characterization: (a) Gradation; (b) Compaction curve.

CONTAINER DESIGN AND CHARACTERIZATION

To accommodate the heavy weight of the rail embankment specimen on the shake table, a light-weight timber container was adopted to extend the areal dimensions of the table and to provide lateral confinement to the soil layers. As timber is not as stiff as a typical steel container used in shake table testing, the container was stiffened and braced to withstand the static stresses associated with compaction and dynamic stresses during shaking. The container configuration is illustrated in Figure 5. The base of the container is supported by four main 3375 mm × 1530 mm Parallam beams which are connected rigidly to the shake table. These beams support a thirteen secondary joists of 102 mm × 102 mm that extend beyond the width of the container. The base of the container was constructed from plywood decking attached to the joists, and 25 mm-thick strips of wood were connected at a 0.3 m spacing to ensure a strong frictional connection between the base of the container and the subgrade layer. The back and side walls were formed from plywood decking. The sidewall decking is supported by a series of 102 mm × 102 mm studs, which are attached using double gusset plates to the joists extending across the base of the container. The goal of these gusset plates is to provide increase the bending stiffness of the side walls to approximate plane strain conditions as closely as possible. The interior surfaces of the side walls were covered with Visqueen plastic sheeting to minimize friction.

Although the centerline of the 2-direction rail embankment shown in Figure 1 is expected to deform like a shear beam as observed in the transverse shake table tests on MSE bridge abutments reported by Zheng et al. (2018), it was not possible to create a laminar container that could allow the backwall of the container holding the half section rail embankment specimen to deform together with the soil due to the unconstrained embankment slope. Instead, the container was constructed with a relatively rigid back wall at the location of the embankment centerline to provide a simple boundary condition to simulate in numerical future simulations. This approach is consistent with the back wall boundary condition used in previous shake table projects on longitudinal shake table tests on MSE bridge abutments (e.g., Zheng et al. 2019). To provide as rigid a back boundary as possible, the back wall is supported by a set of studs fixed to the base as well as a pair of wailers attached to the sidewalls. As significant inertial forces are expected on the back wall in the direction of the motion, tension bars and studs were used to connect the middle of the back wall to the base studs. The front face of the container is open so that the slope face of the embankment can deform freely.

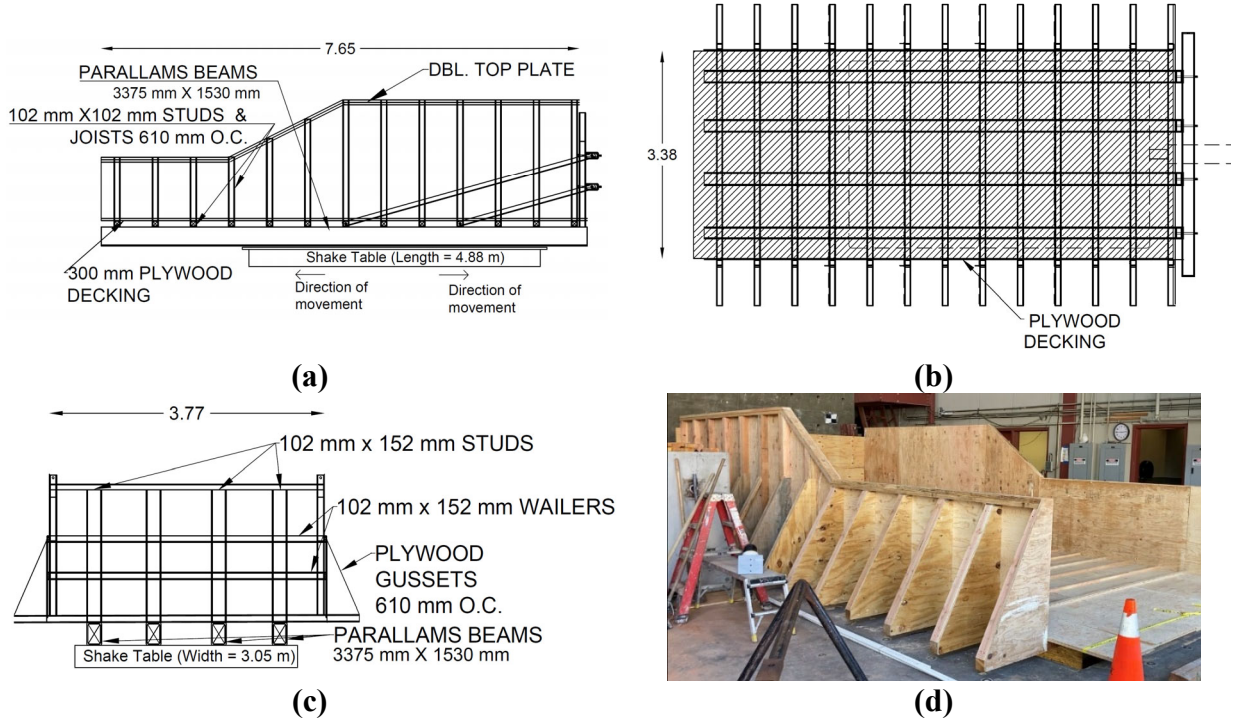

Figure 5. Container for shake table testing of full-scale rail embankments: (a) Side view, (b) Plan view, (c) Back view, and (a) Picture of completed container.

INSTRUMENTATION

A schematic showing instrumentation in the rail embankment specimen is shown in Figure 6(a). The horizontal motion of the container is measured by 2 string potentiometers (P01 and P02) and 2 accelerometers (A01 and A02). The horizontal displacement of the rails is monitored by string potentiometers (P03 and P04). Spring-loaded linear potentiometers were placed vertically at the end of each rail on a sliding plate to measure the rail settlements. Potentiometers P07 and P08 are used to monitor Rail 1 while potentiometers P05 and P06 are used to monitor Rail 2. Vertically- and horizontally-oriented accelerometers (A03 and A04, respectively) were also placed on Rail 1.

The string potentiometers were Model P-5A/15A/25A/30A/40A from Rayelco, the linear potentiometers were Model 606 from BEI sensors, and the accelerometers were Model CXL02LF1 from Crossbow. Although not reported in this paper, settlement plates were incorporated to measure settlements at different depths in the embankment under and outside the rails, sensors to measure the deformation of the slope at the crests of the ballast and the subballast, and earth pressure cells oriented horizontally along the back wall. Aluminum rails were mounted across the top of the box to mount instrumentation, as shown in Figure 6(b). A detail of the rail-wall connection developed to promote in-plane deformation behavior is shown in Figure 6(c), along with a linear potentiometer (before reorientation to measure vertical movements of the rail).

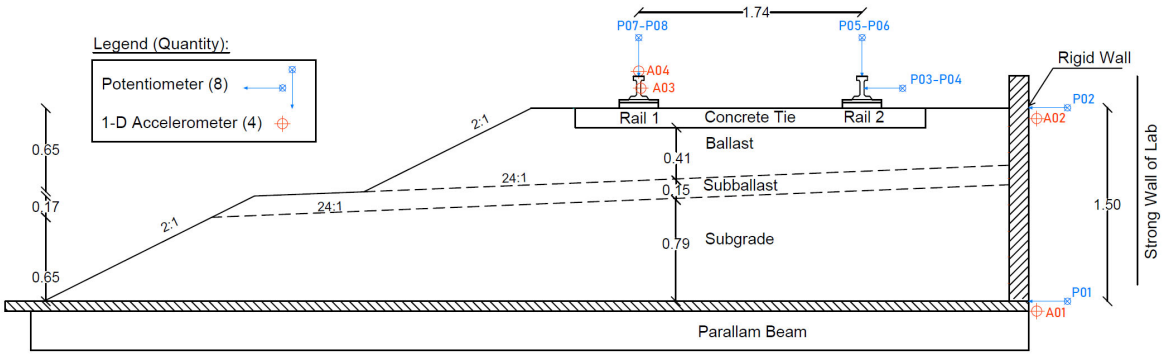

(a)

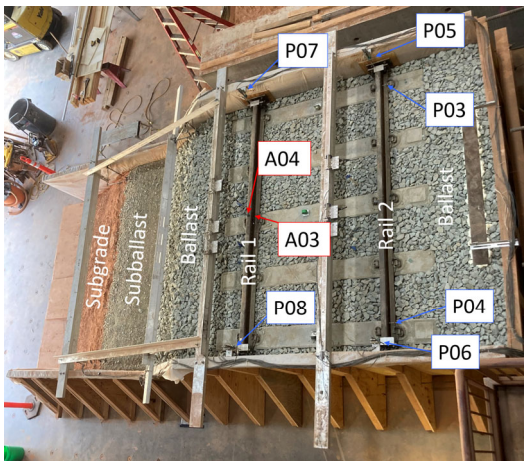

(b)

(c)

Figure 6. Instrumentation layout: (a) Plan of representative section, and (b) Constructed rail embankment after instrumentational placement; (c) Rail-wall connection detail.

APPLIED EARTHQUAKE MOTIONS AND CONTAINER RESPONSE

After construction of the rail embankment specimen, a series of earthquake motions and sinusoidal motions with different frequencies were applied. Although the shake table could be operated in displacement or acceleration control, experience with previous studies involving heavy payloads on the UCSD Powell Laboratory shake table (e.g., Zheng et al. 2018, 2019; Zayed et al. 2020) indicate that the shake table performs better when operated in displacement control. Before each applied earthquake or sinusoidal motion, a white noise motion with small amplitude was applied to the rail embankment specimen for system identification as permanent deformations may lead to

a change in the dynamic deformation response. The applied earthquake motions considered in this study were records from the Gilroy Station 2 and the Corralitos stations recorded during the 1989 Loma Prieta earthquake. During the full testing program, the amplitude of the applied motion (in terms of displacement) was increased in increments from 25% to 150%. The 1989 Loma Prieta seismic event generated significant effects on the San Francisco Area and the two records mentioned above have different predominant frequencies that allow evaluation of the effect of this variable on the deformation response of the embankment.

Before constructing the embankment within the container, the behavior of the empty container was characterized. A comparison of the achieved displacements at the top and base of the container with the Gilroy Station 2 record at full scale (abbreviated as Gilroy-100%) is shown in Figure 7(a). These displacement results indicate that the shake table can replicate the record well in terms of displacement, and that the top and bottom of the container move together as a rigid body. A comparison of the accelerations measured at the top and bottom of the container are shown in Figure 7(b). The results show that the base of the empty container generates a similar record compared to the actual earthquake record but that the top of the box amplifies the acceleration record by about 280% which indicates that the back of the container is not completely rigid and acts as a restrained cantilever beam when the container is empty.

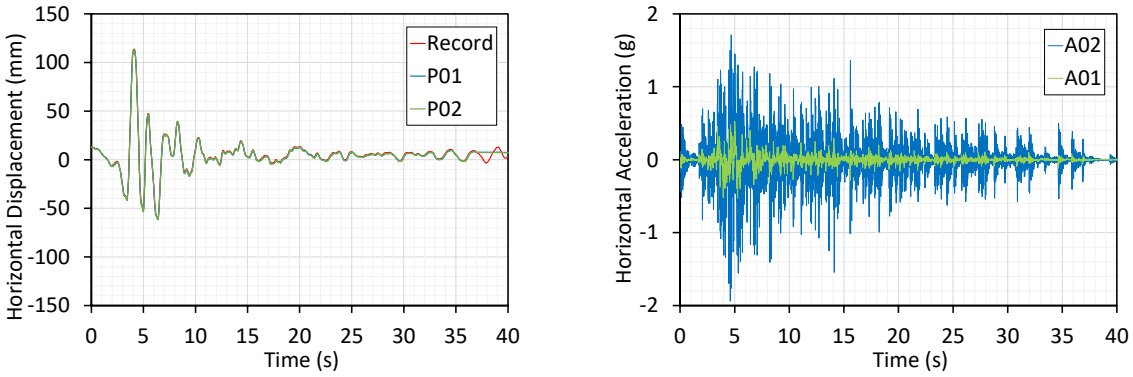

(a) **(b)**

Figure 7. Empty container characterization: (a) Displacements from Gilroy-100% motion with those measured at base and top; (b) Accelerations at base and top

CROSSLEVEL VARIATION RESULTS

Although several earthquake motions were applied to the rail embankment specimen, this paper presents the key deformation and acceleration results from a test with the Corralitos record scaled by 125% (abbreviated as Corralitos-125%). A comparison of the measured displacement at the base of the box and the applied record is shown in Figure 8(a). Because the record has a large movement in the positive direction (away from the actuator) in the first 3 seconds, the table was first shifted by -50 mm toward the actuator before the motion was applied and time was permitted for all sensors to stabilize. The results in Figure 8(a) indicate that the shake table was able to capture the earthquake record well even with the heavy payload of the embankment specimen. Very small offsets are observed when direction changes occur during shaking. The results from accelerometer A01 at the base of the container, which represents the applied earthquake motion, and the results from accelerometer A04 on Rail 1 are shown in Figure 8(b). An amplification of 1.14 is observed at the level of Rail 1, which is less than that noted at the back wall of the empty

container. For the Corralitos-125% motion, the measurements from accelerometer A01 show a peak acceleration of about 1.05 g, along with a significant number of cycles with peaks of 0.25 g. Spectral acceleration response curves were calculated from the actual earthquake record and from the acceleration time record measured at the base of the container, as shown in Figure 9. The response spectrum for the record shows a dominant period of 0.35 s. While the response spectrum for the measured acceleration at the base of the container also shows a peak at this period, there are also several additional modes at lower periods with more energy, with a dominant period of 0.163 s. This lower dominant period may be due to the characteristics of the shake table and the control system. As a comparison, the response spectrum calculated from the white noise motion applied before the Corralitos-125% motion is also shown in Figure 9. This motion indicates that the fundamental frequency of the rail embankment specimen is 0.138 s. This is close to the dominant frequency of the measured acceleration at the base of the container. This indicates that partial resonance is expected during application of the Corralitos-125% motion to the embankment specimen. The response spectra were calculated assuming a damping ratio of 1%.

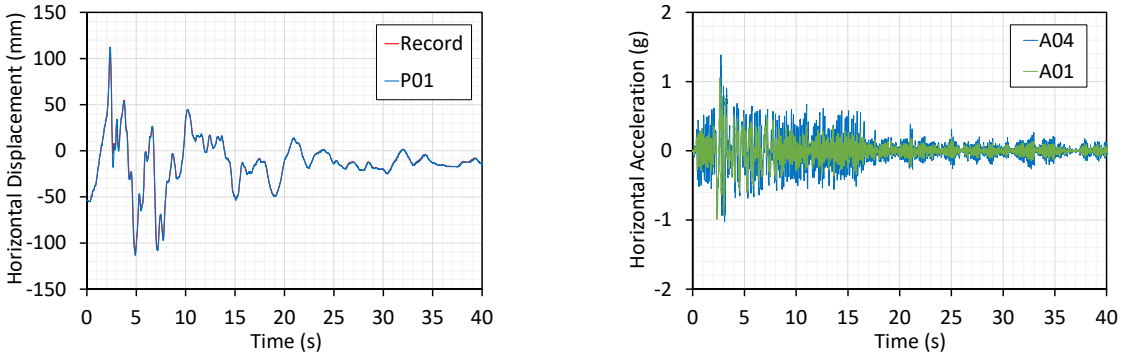

(a) **(b)**

Figure 8. Comparison of time-histories measured during application of the Corralitos-125% motion to the embankment specimen: (a) Displacements from the record and those measured at the container base, and (b) Accelerations measured at base and Rail 1.

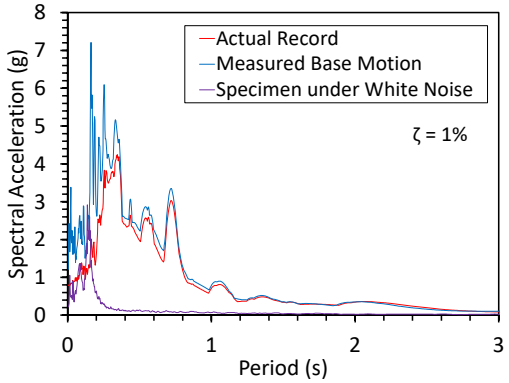

Figure 9. Spectral acceleration relationships calculated from the applied record and achieved base motions along with that from Rail 1 during a white noise shake

The incremental CLV during shaking is calculated from the difference in the average transient settlements of Rails 1 and 2. Time series from potentiometers P07 and P08 used to measure the settlement of Rail 1 are shown in Figure 10(a), while time series from potentiometers

P05 and P06 used to measure the settlement of Rail 2 are shown in Figure 10(b). Positive settlements are defined as downward. While it was expected that the rails would settle by the same amount at both ends of the container if plane strain conditions were ensured, the flexibility of the container and possible initial differences in the contact between the rails/ties and the ballast across the width of the box may have led to the differences in rail settlement across the container during shaking. The average settlement of each rail was used in calculation of the cross-level variation. Evaluation of the settlement time series in Figures 10(a) and 10(b) indicates that an initial heave occurred when the motion experienced the rapid displacement at the beginning of the test, after which the rails gradually settled throughout the remainder of the motion. This is confirmed when plotting the average settlement of each rail versus the horizontal displacement of the rails in Figure 10(c). A large heave (negative settlement) is observed after the initial large positive displacement, after which a gradual shakedown is observed for the rest of the motion that predominantly occurs in the negative displacement regime. Finally, the results for CLV are shown in Figure 10(d), where a positive CLV implies that Rail 1 settles more than Rail 2.

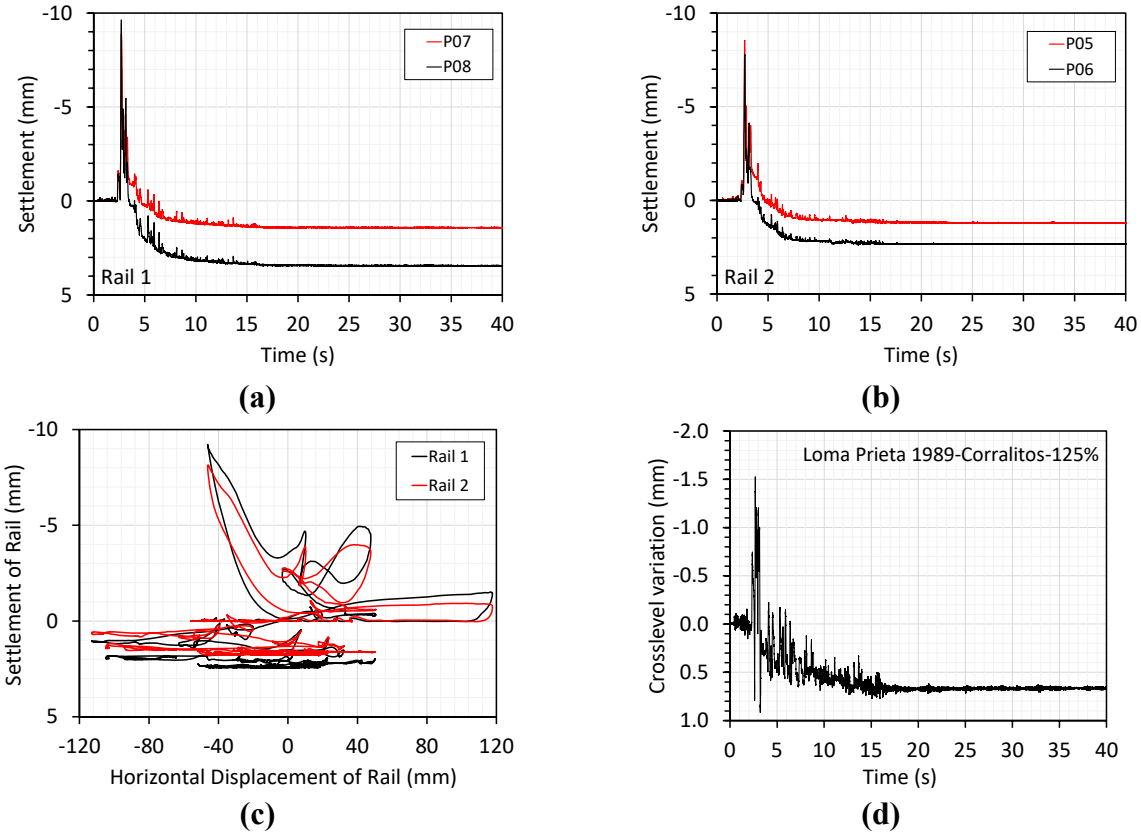

Figure 8. Shake table records: (a) Rail 1 vertical displacements; (b) Rail 2 vertical displacements; (c) Horizontal vs. vertical displacements; (d) Cross-level variation.

Overall, the results indicate that Rail 1 settles more than Rail 2, possibly because of the lower confinement near the unconstrained slope of the embankment. However, the residual CLV at the end of shaking is only 0.66 mm for this motion, which is 3.46% of the BART limit of 19.05 mm for Class 5 track. This small CLV indicates that the rail embankment specimen performed well under the applied earthquake motion, which had a high peak horizontal acceleration and a dominant frequency that is close to the predominant frequency of the rail embankment. While the

CLV from embankment deformations is small, it is possible that the natural soil underlying the embankment may settle differentially during shaking, translating into higher CLV.

CONCLUSIONS

This paper presents results from a shake table test performed to characterize the deformation response of a full-scale ballasted rail embankment with geometry representative of BART rail infrastructure. For an example shake table test with an applied motion from the 1989 Loma Prieta Corralitos record scaled to 125% of its peak displacement amplitude the residual cross-level variation between the two rails of the track was 0.66 mm, which is less than the most restrictive threshold of 19.05 mm set by BART, even though the horizontal acceleration at the level of the rails was as high as 1.2 g. Additional testing is being underway to develop a relationship between different characteristic of earthquake motions and cross-level variations of rail embankments.

ACKNOWLEDGEMENTS

Support for this study provided by Bay Area Rapid Transit (BART) under agreement 6M3466 is gratefully acknowledged. The authors thank Chung-Soo Doo and Carlos Rosales of BART for their support. The authors also thank Andrew Sander, Noah Aldrich, Michael Sanders and Darren McKay for their input and support during construction and testing of the specimen.

REFERENCES

ASTM. (2000). *Standard Test Methods for Laboratory Compaction Characteristics of Soil Using Standard Effort*. ASTM D698-00a, West Conshohocken, PA

ASTM. (2017). *Standard Test Method for Bulk Density ("Unit Weight") and Voids in Aggregate*. ASTM C29/C29M - 17a, West Conshohocken, PA.

BART. (2009). *BART Facilities Standards*, Sections 31 00 00 and 34 11 27.

Housner, G. W., and Lili, X. (2014). *Report on the Great Tangshan Earthquake of 1967, Ch. 1. Railway Engineering*. Earthquake Engineering Research Lab. Caltech. Pasadena, CA.

Nakamura, T., Sekine, E., and Shirae, Y. (2011). "Assessment of aseismic performance of ballasted track with large-scale shaking table tests." *QR of RTRI*. 52(3), 156-162.

Sogabe, M., Asanuma, K., Nakamura, T., and Kataoka, H. (2013). "Deformation behavior of ballasted track during earthquakes." *QR of RTRI*. 54(2), 104-111.

Trautner, C., Zheng, Y., McCartney, J. S., and Hutchinson, T. (2017). "An approach for shake table performance evaluation during repair and retrofit actions." *Earthquake Engineering and Structural Dynamics.* 47, 131-146.

Zayed, M., Ebeido, A., Prabhakaran, A., Kim, K., Qiu, Z., and Elgamal, A. (2020). "Shake table testing: A high-resolution vertical accelerometer array for tracking shear wave velocity." *Geotechnical Testing Journal*. 44(4), 1-22.

Zheng, Y., McCartney, J.S., Shing, P.B., and Fox, P.J. (2018). "Transverse shaking table test of a half-scale geosynthetic reinforced soil bridge abutment." *Geosynthetics International*. 25(6), 582-598.

Zheng, Y., Fox, P.J., Shing, P.B., and McCartney, J.S. (2019). "Physical model tests on half-scale geosynthetic reinforced soil bridge abutments. II: Dynamic loading." *ASCE Journal of Geotechnical and Geoenvironmental Engineering*. 145(11), 04019095.